

new travelling wave coil concepts

M. Mueller¹, R. Umatham¹, S. Alt¹, W. Semmler¹, and M. Bock¹

¹Medical Physics in Radiology, German Cancer Research Center (DKFZ), Heidelberg, Germany

Introduction

Travelling wave MRI can be used to attenuate the standing wave problem of volume resonators [1] at high magnetic field strengths. Classic travelling waves lead to high global SAR and electromagnetic wave reflection in head and shoulder areas, or at the lower extremities. In this work, we introduce two new travelling wave RF coil designs utilizing stripline concepts which solve these problems by exciting the RF field just where it is needed, at the investigation area (IA). We evaluate these coils by FDTD simulations, and investigate their usability by simulations with a detailed anatomical model [2].

Materials and Methods

The travelling wave RF coils are designed to expose only a well defined region of interest (ROI) of the body to the RF field, thus the whole-body SAR remains limited. The TX/RX coil dimension is variable, so that it can be operated as a local coil or act as a whole body coil. By design, the coils have no cut-off frequency as other travelling wave approaches [1], and can thus operate at multiple frequencies (e.g., for multi-nuclear MR).

Both travelling wave coils V1 and V2 are based on a 16-channel stripline coil design in circular arrangement (Fig.1). For comparison both coils are designed with equal dimensions (length: 30cm; outer diameter: 39 cm; inner diameter: 34 cm) with 16 striplines (diameter of outer layer: 38cm; width of outer layer: 6.46 cm; length: 29 cm; isolation gap: 1cm). While V2 has continuous striplines, V1 has an intermitted inner conductive layer (diameter: 34 cm; width: 5.68 cm; isolation gap: 1 cm), which is defined as ground plane (Fig. 1). In V2 the striplines are filled with a dielectric (acrylic glass, $\epsilon_R = 2.6 \text{ Fm}^{-1}$ at 297 MHz) to concentrate the E -field between the striplines. At V2 the outer stripline layer is defined as ground plane and the continuing inner strips are smaller (diameter: 38 cm; width: 2.68 cm; length: 29 cm) to facilitate higher B_1^+ field strength in the center.

At both coils the travelling RF waves are coupled into each stripline via an impedance-matched port and terminated at the other end by matched impedances. All adjacent striplines have a phase difference of 22.5° . Thus, the stripline arrangement is circularly polarized. A conductive shield focuses the RF field at the inside of the coil. For the simulations a cylindrical phantom (diameter: 28cm; length: 1m) was placed in the coils. The dielectric parameters were set to the average human tissue characteristics at 297 MHz ($\epsilon_R = 52 \text{ Fm}^{-1}$; $\sigma = 0.7 \text{ m/s}$) [3,4]. Size and dielectric parameters of the phantom resemble the load of a human abdomen. RF field calculations were performed with the software package SEMCAD X V14.2 (Speag, Zürich, Switzerland) using a discretization grid size of 25 million cells (phantom), 200 million cells (Ella, a virtual family model) and 15 periods of harmonic transmission at 297 MHz (Larmor frequency at 7 T). The B_1^+ field distribution was evaluated and SAR calculations were performed according to IEEE-1529. At both coil designs S11 (port-side) was lower than -21 dB and S22 (termination-side) was lower than -50 dB.

Results and Discussion

Simulations show a focusing of the RF field to the IA (Figs. 2 and 4). While the IA is completely B_1^+ covered the SAR is restricted to the IA. The B_1^+ field distribution is smooth in longitudinal direction (Fig. 3). A maximum B_1^+ field variation in longitudinal orientation over a distance of 15cm/20cm of 14.8%/24.6% (V1) and 10.3%/22.4% (V2) is reached. In transversal orientation the B_1^+ signal is attenuated towards the center of the phantom, but has a local maximum at the central axis caused by constructive interference of the B_1^+ field vectors. Since both coil designs have a similar B_1^+ field distribution, especially in transverse orientation, the B_1^+ and SAR distributions were normalized by their respective B_1^+ peak values. Interestingly, the SAR characteristics of both coils are also similar. Both decay towards the phantom center due to dielectric losses and have a stronger decay at the center due to constructive interference of the E -field vectors. Outside the IA SAR rapidly declines in longitudinal direction. 10 cm outside the coil the SAR decreases by 95-98% (V1) and 98.7-99.9% (V2) in relation to the SAR in the IA.

Conclusion

Simulations show that both travelling wave stripline coil designs perform for MRI. Interestingly, design differences of the implementations have only a small, effect on the B_1^+ and SAR distribution. Nevertheless, both stripline coil designs show a good homogeneity and the positive aspect of an increasing B_1^+ but a decreasing SAR at the center of the phantom (transversal). It is feasible to use these stripline designs to improve the standing wave problem, to focus the RF energy to the region of interest and to keep whole body SAR low.

[1] Brunner et al, Nature 2009 457(7232)

[2] Christ A et al, Phys Med Biol;55(2):N23-38.

[3] Gabriel C, Gabriel S et al, Phys Med Biol 1996;41(11):2231-2293

[4] <http://www.fcc.gov/oet/rfsafety/dielectric.html>

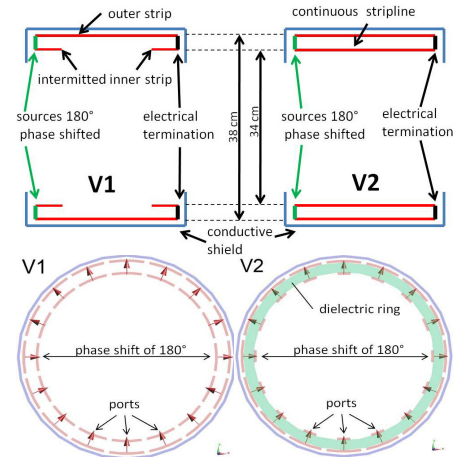


Fig.1: Stripline coil design V1 and V2 in cross section view (top) and front view (down) without frontal shield cover.

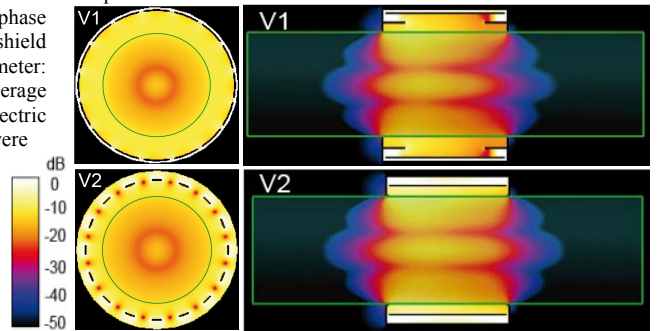


Fig. 2: B_1^+ field distribution of transversal (left) and coronal (right) slices through the phantom center. The phantom is indicated by the green circle/rectangle.

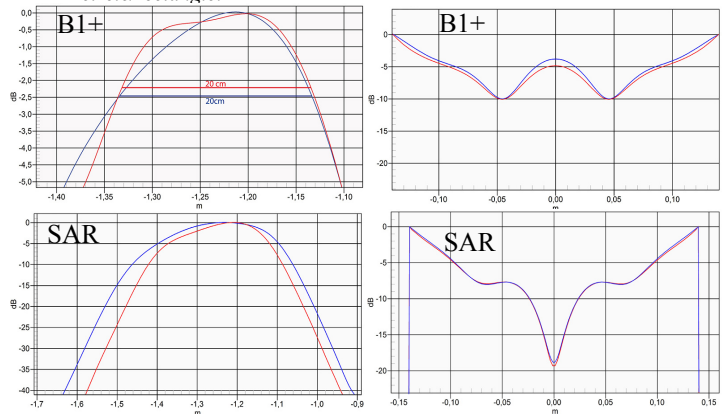


Fig.3: longitudinal (left) and radial (right) line plots through the phantom center of V1 (blue) and V2 (red).

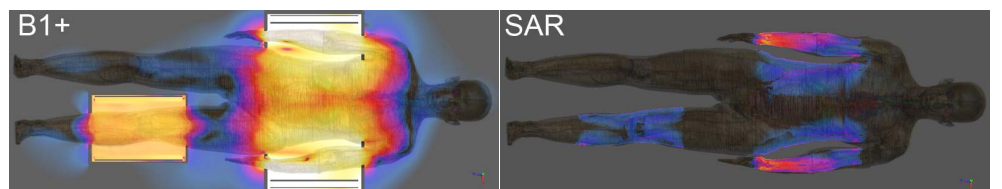


Fig.4: B_1^+ and SAR field distribution of the central coronal slice of the human abdomen (Ella) and knee, using a body coil and a local TX/RX- knee coil, both in stripline V2 design (same color map as in Fig. 2).